View metadata, citation and similar papers at core.ac.uk
brought to you by CORE
provided by TU Delft Open Access Journals

Diagnostics Based on Acoustic Distributed Sensor Data and Machine Learning

Dennis Struver
Eindhoven University of Technology
d.p.p.struver@student.tue.nl

Wouter Weekers
Eindhoven University of Technology
w.weekers@student.tue.nl

ABSTRACT
Accurate real-time diagnostics of high-tech systems are becoming more and more important. Therefore, the potential of distributed acoustic sensors in combination with machine learning for contactless diagnostics of machine performance has been investigated. Hereto, frequency response data of a brass plate has been gathered through experiments and a finite element model. In order to investigate the possibility of identifying the locations and weight of the masses, Support Vector Machines and Random Forest algorithms have been trained with experimental and numerical data. The Random Forest algorithm shows promising performance with short computational time, easy application, 95% accuracy and relatively easy understandability.

Keywords
Diagnostics, acoustic emission, vibration sensor data, machine learning, support vector machines, random forest.

INTRODUCTION
Machine learning is recently being used more and more in different fields of research. In the field of dynamics, machine learning could bring plenty of improvements as well. For example, real-time contactless diagnostics of high tech systems. Real-time detection of irregularities in these systems is necessary for long-term and safe operation. Ideally monitoring would happen without interrupting the operation of the machines, to keep the downtime as low as possible. To this end, an acoustic sensor would be a great improvement, enabling the possibility to monitor the behavior and performance of multiple parts. This paper aims to develop such methodology for detecting irregularities in structures or systems, using machine learning algorithms trained with data obtained from acoustic measurements and a finite element model. For this purpose, the frequency response of a basic plate structure has been investigated. Small masses have been used to represent structural irregularities and one normal mode has been observed in particular. This mode is depicted in Fig. 1, where the minus and plus signs represent displacement in and out of the page respectively. This mode shows 9 clear sectors and thus makes it possible to monitor the changes of 9 extrema separately.

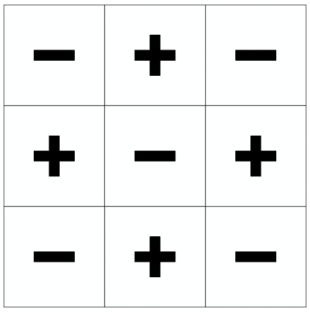

Fig. 1: The mode shape of interest. Here '−' and '+' denote displacements in and out of the page respectively.

'Permission to make digital or hard copies of all or part of this work for personal or classroom use is granted under the conditions of the Creative Commons Attribution-Share Alike (CC BY-SA) license and that copies bear this notice and the full citation on the first page''
SRC 2018, November 9, 2018, The Netherlands.

THEORY
First, in order to understand the dynamical behavior of a plate, and the corresponding sound generation and detection, the relevant theory is elaborated.

Plate vibrations
A natural vibration is defined as the free motion that will follow when an arbitrary initial disturbance, i.e. excitation, is imposed on an undamped time-invariant single-degree-of-freedom linear system. Such a natural vibration indicates that the system vibrates at a so-called natural frequency, which depends on the system parameters. Each natural frequency corresponds to a certain configuration of the system's motion, called a normal mode, e.g. the mode shape shown in Fig. 1. For an undamped multi-degree-of-freedom linear system, its free motion is a superposition of all its normal modes. Analytically, the natural frequencies and modes can be obtained by using the equations of motion to solve the algebraic eigenvalue problem [1].

Sound generation and detection
In sound generation, bending waves are the most important and induce a displacement of the particles that is mainly perpendicular to the plate's surface. These sound waves can be recorded with a receiver, which makes it possible to identify the sound pressure or intensity. Moreover, it is possible to separate a sound wave into its component parts, which are various sound wave frequencies and noise. From this, the frequency of each of the different sound wave components can be determined, which are the different natural frequencies. Additionally, at a fixed distance from the source, the pressure, velocity, and displacement of the medium vary in time. On the other hand, at an instant in time the pressure, velocity and displacement vary in space. The transversal displacement caused by the bending waves is proportional to the particle velocity in the direction perpendicular to the plate. Thus, with multiple receivers, it is possible to detect the complete motion of the plate, since every receiver detects the plate's motion at a specific location.

EXPERIMENTS
To gather experimental training data, a considerable amount of measurements has been performed in a semi-anechoic chamber. The experimental set-up consisted of a vertically oriented brass plate of dimensions 0.401 x 0.401 x 0.002 [m] and mass 2.67 [kg], positioned parallel to a microphone array as shown in Fig. 2. The distance between the array and the plate has been chosen as $z_d = 30$ [mm].

Each corner of the plate has been attached to the aluminum frame by deflated bicycle inner tubes. The array that has been used is a CAM1K Sorama microphone array with 1024 microphones in a 32 by 32 grid. The plate has been excited manually using a hammer equipped with a nylon tip. With an impact excitation it has been ensured that the dynamical behavior of the plate is not influenced and thus a natural vibration is induced.

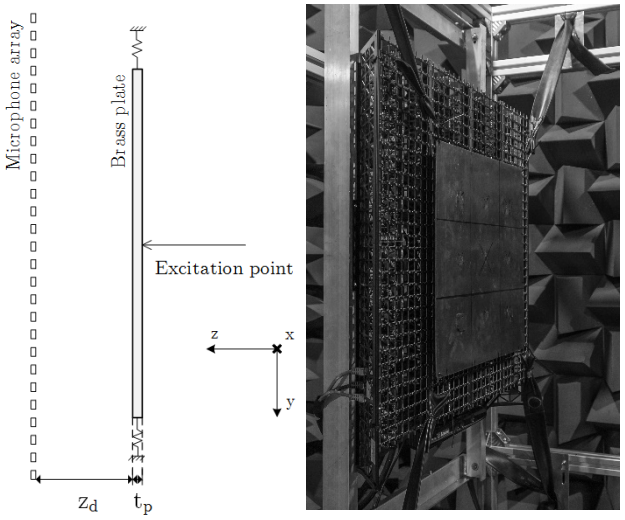

Fig. 2: Schematic representation (left) and picture (right) of the experimental set-up.

The mode of interest that has been used for this paper contains 9 sectors. The extrema in de mode shape are located somewhat closer to the middle of the plate and thus, the plate has been divided into 9 equal sectors, according to the nodal lines around the extrema. Small plate masses of 20 and 60 [g], respectively 0.75 and 2.25% of the total mass, have been used to represent irregularities in the plate. The masses have been attached to the midpoint of a sector using beeswax. The location and numbering of the sectors and location of the masses and excitation point are shown in Fig. 3.

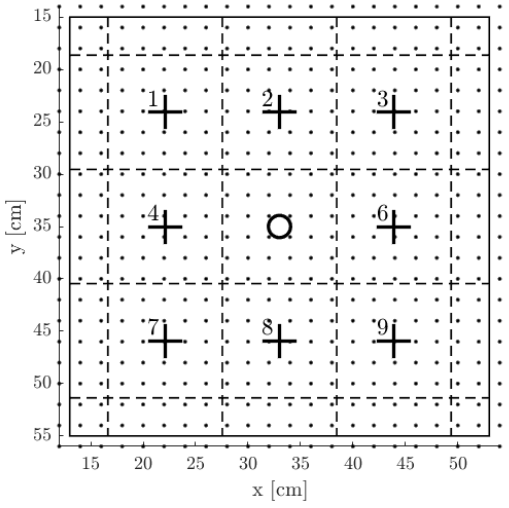

Fig. 3: Sector and mass locations. The continuous line marks the plate. '+' indicate the mass locations with corresponding sector number, dots indicate microphone locations, dotted lines mark the sectors and the circle shows the point of excitation.

For each sector, except for sector 5 due to the excitation point being located there, 20 measurements per mass, both 20 and 60 [g], have been performed. Moreover, 20 measurements for the clean plate, without mass, have been done. For some randomness and small deviations in the results, a maximum of 5 consecutive measurements has been done, after which the mass has been repositioned. The measurement data has been processed using MATLAB and its implemented Fast Fourier transform (fft) function, to obtain the acoustic data corresponding to the mode of interest. The acoustic field at the hologram plane (microphone array), is different from the one at the source plane (vibrating plate). A reconstruction, i.e. acoustical holography, could be applied to solve this. However, as proven by Moers (2016) [2], this has a negligible effect on the amplitude, and therefore, the shape of the modes. Hence no reconstruction has been applied. To be able to compare the resulting sound pressure images, the pressure data has been normalized to a maximum value of unity. For completeness of the sound image, the normalized values are multiplied with the sign of the real part which makes it possible to distinguish positive and negative extrema.

As an example, the sound image of a measurement with 60 [g] in sector 1 can be seen in Fig. 4. This sound image proves that the mode shape shows clear indications about the location of the mass, making it possible to identify an irregularity from the acoustic data.

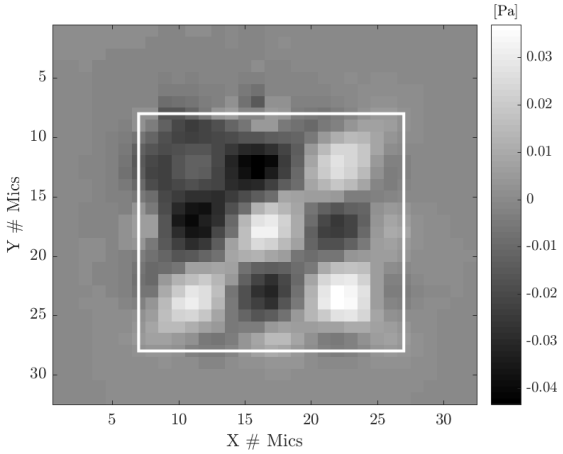

Fig. 4: Sound pressure image for a measurement with 60 [g] in sector 1. The white square marks the plate position.

FINITE ELEMENT MODEL

To generate more training data without having to perform the experiment, a finite element model has been made in ANSYS. First, quadrilateral elements of the Serendipity type have been used to mesh the model. Material properties have then been assigned to the mesh. The density ρ of 8100 [kg/m^3] has been found by weighing the plate. Furthermore, the Poisson's ratio ν has been chosen as 0.33 [-], which is a typical value for brass, and the Young's modulus E has been tuned such that the mode of interest matches the frequency of the one found in the experiments, resulting in 92.3 [GPa]. Finally, a damping ratio ζ of 0.00137 [-] has been found using the 3 dB-bandwidth method defined as

$$\zeta = \Delta f / f_0 ,$$

where f_0 is the frequency of the mode of interest in the experiment and Δf is the distance between the frequencies for which the response is 3 dB lower.

It has been found that free-free boundary conditions represent the boundary conditions from the experiment

best. Finally, the masses have been simulated using point masses placed on the node closest to the point (x,y) where

$$x = x_c + r\cos\theta$$
$$y = y_c + r\sin\theta.$$

Here, (x_c,y_c) is the location of the mass, as shown in Fig. 3. During each of the 30 simulations per sector, r and θ have been randomly sampled from uniform distributions ranging from 0 to 1 [cm] and 0 to 2π [rad] respectively, in order to generate randomness in the location for the mass. This randomness results in slightly different responses, which is necessary to train the algorithms. In each simulation the plate has then been excited in its center using a unity force. For simulations of the plate without mass, the location of the excitation force has been changed around the center of the plate in the same manner as the location of the mass. The response of the plate has then again been normalized in the same way as with the experiments, to be able to compare the two responses. This comparison has been done using the Modal Assurance Criterion (MAC) defined as

$$MAC = \frac{|\phi_M^T \phi_E|^2}{(\phi_M^T \phi_M)(\phi_E^T \phi_E)},$$

where ϕ_M and ϕ_E represent modal vectors of the model and the experiment respectively. From this equation follows that when the two modes are equal, the MAC equals 1. For the considered plate and model, the MAC has been found to be only 0.60. However, looking at Fig. 5 the main difference is located at the edge of the plate, where the soundwaves detected by the microphones are weaker as they can diffuse more in all directions. When excluding the edges of the plate, a MAC of 0.94 has been found. Therefore, it can be concluded that the model is accurate when the edges are excluded, hence the edges are not considered in further analysis.

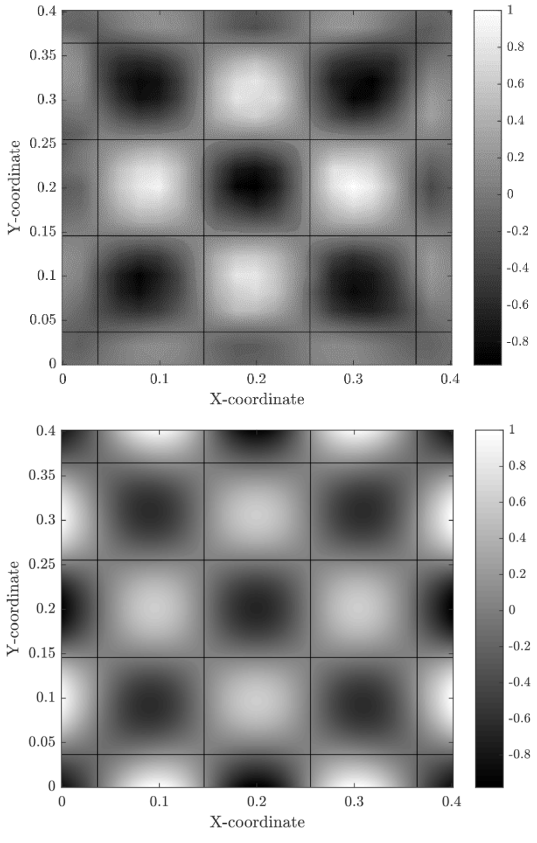

Fig. 5: Normalized response of the plate for the experiment (top) and the model (bottom).

DETECTION ALGORITHM

Using the data from the experiment and the model, two types of machine learning algorithms are investigated: Support Vector Machines (SVM) and Random Forest (RF). These algorithms are chosen for their understandability, ease of implementation and their classification performance in other applications.

Support Vector Machines

SVM make binary classifications by assigning a value of +1 or -1 to each class. Classification of an input a then happens according to the function

$$g(a) = sign\big((w \cdot a) + c\big).$$

Here, w is a vector of weights and c is a bias, which are found by means of a minimization problem during training of the algorithm. If classification in more than two classes is desired a *one-versus-one* or *one-versus-all* approach can be taken, which specify one class as the positive class and one or all other classes as the negative class, respectively. In [3] the inner working of the SVM are explained in more detail. Optimization of several other parameters of the SVM can be performed automatically in MATLAB. This uses Bayesian optimization and has high computational time. More information regarding the parameters to be optimized and the theory behind the Bayesian optimization in MATLAB can be found in [4].

Random Forest

RF makes classifications by taking the majority vote of several decision trees. These trees are directed graphs with randomly chosen parameters, such as its maximum depth, which are 'grown' during the training of the algorithm. This growing procedure aims to minimize the impurity of each node defined using the Gini index as

$$i = 1 - \sum_j p^2(j)$$

where p is the fraction of class j present at a given node. Optimization of the RF can be performed by changing the number of trees. A more detailed explanation of the RF can be found in [5].

Algorithm accuracy results

Both algorithms have been implemented in MATLAB, using the *fitcecoc* and *TreeBagger* functions, to identify the sector in which the mass is located and the weight of the mass from the response of the plate. Furthermore, the influence of the amount of experimental training data on the performance has been investigated. Minimizing this amount, while maintaining reasonable accuracy, reduces the amount of physical experiments needed to train an algorithm, which is preferred for more advanced systems. First, the experimental data has been interpolated to a finer grid that matches the numerical element grid. After that, the pressure data is squared in order to eliminate the sign dependency. This data is then divided into 9 sectors and converted to a ratio I by

$$I_S = \frac{\sum_n v_{S,n}^2}{\sum_s \sum_n v_{s,n}^2}$$

where S denotes the sector for which I is calculated, n denotes all nodes in sector S, s denotes all individual sectors and v is the normalized response of a node. This data has been used to train the algorithms, which could then distinguish test data by sector number and weight of

the mass. Both algorithms have been trained with 25 measurements per mass, per sector, randomly chosen from the gathered data set. This means that a total of 425 measurements have been used to train the algorithms and 17 classes can be distinguished. Furthermore, the ratio between experimental and numerical data has been varied and expressed as a percentage of experimental data out of the total training data. Once trained, the algorithms have been tested with 5 measurements per mass, per sector, randomly chosen from the data not used for training. Performance on experimental and numerical data have been tested separately. The accuracy is then expressed in the percentage of correct classifications out of all classifications made. In Fig. 6, the performance of the optimized SVM and the RF with 20 trees on experimental data are shown. It can be seen that the change of performance is similar in shape, with the RF performing slightly better. For the optimized SVM, an accuracy of 95% is reached at approximately 40% of experimental training data, whereas for the RF the 95% accuracy is reached at approximately 20% of experimental data. In Fig. 7, the performance of the optimized SVM and RF algorithm on numerical data is shown. Here, it can be seen that the performance is more than reasonable for both algorithms. A small difference in performance can be seen for the optimized SVM, as the accuracy slightly decreases when adding more experimental training data, whereas the RF performs rather stable at around 100%.

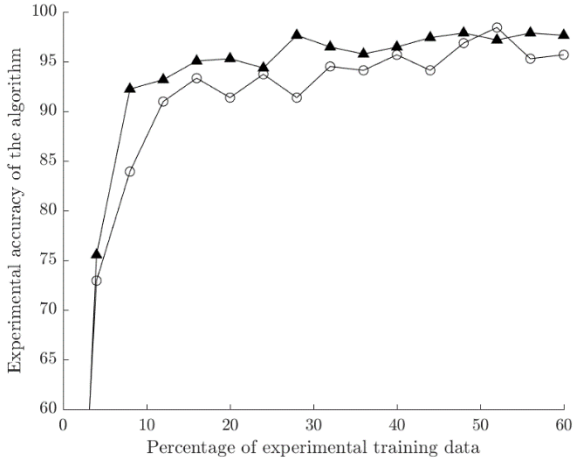

Fig. 6: Accuracy of the optimized SVM (○) and RF (Δ) when classifying experimental data.

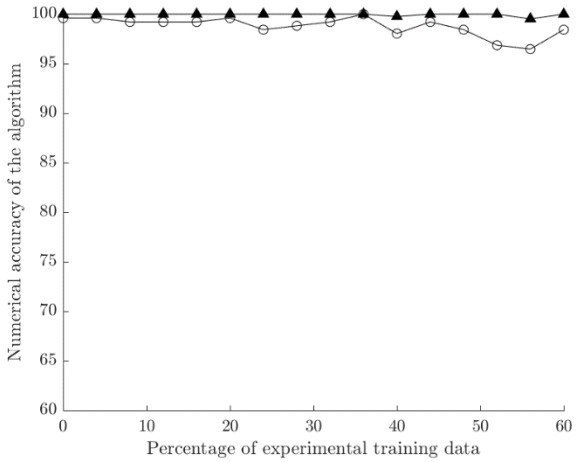

Fig. 7: Accuracy of the optimized SVM (○) and RF (Δ) when classifying numerical data.

CONCLUSION

For this paper acoustic experiments have been performed on a basic plate structure, to which masses have been added to simulate irregularities. Furthermore, a finite element model representing this plate has been developed. It has been shown that this modeled plate, when excluding the edges, accurately describes the plate used in the experiments. Response data resulting from excitation of the plate and the finite element model has been used to train two machine learning algorithms for detecting the location of the added mass and its weight. The used algorithms, Support Vector Machines and Random Forest, both reached over 95% accuracy using respectively 40% and 20% data from the physical experiments in the training set. Moreover, it has been found that the Random Forest reaches a higher overall performance. An additional benefit of the Random Forest is its simplicity regarding both understanding the algorithm, as well as optimizing it leading to lower computational times. Therefore, it has been concluded that for a similar classification purpose, the Random Forest is the better algorithm to use.

Improvements could be made in further research, by using holographic reconstruction of the image of the plate to verify the aforementioned assumption that stated that the difference between the hologram plane and source plane is negligible for the mode shape. Furthermore, the training of the algorithms could be extended by using more modes, which could make it possible to determine the mass location more exactly. Finally, improvements to the algorithm could be made by training it with more data.

ROLE OF THE STUDENT

D. Struver and W. Weekers were both Bachelor's students supervised by I. Lopez Arteaga and I. Rodrigues, when performing the described research. The subject and the mode shape of interest, together with the mass locations, were proposed by the supervisors. Building the experimental set-up, performing the physical experiments and processing its data has been performed by Struver. Developing and validating the finite element model, and processing its data has been done by Weekers. Developing the algorithms, deriving conclusions and writing the paper has been performed by Struver and Weekers together.

ACKNOWLEDGMENTS

We would like to thank both our supervisors, I. Lopez Arteaga and I. Rodrigues, who were always very willing to answer our questions and provide us with helpful feedback.

REFERENCES

1. B. de Kraker, "Mechanical Vibrations". *Shaker*, 2009, ISBN: 9789042303676
2. E.M.T. Moers, "Towards real-time detection of plate vibrations from acoustic measurements", 2016.
3. M.A. Hearst, S.T. Dumais, E. Osuna, J. Platt, and B. Scholkopf, "Support Vector Machines", *IEEE Intelligent Systems and their Applications*, vol. 13, no. 4, pp. 18-28, 1998, ISSN: 1094-7167. DOI: 10.1109/5254.708428.
4. MathWorks. "Documentation fitcecoc". *https://nl.mathworks.com/help/stats/fitcecoc.html,* 2014. [Accessed on 24 May 2018].
5. G. Louppe, "Understanding Random Forests: From Theory to Practice", 2014. arXiv: 1407.7502 [stat.ML]